

Supporting Information

Evaluation of P3-type layered oxides as K-ion battery cathodes

Pawan Kumar Jha[†], Sanyam Nitin Totade[‡], Prabeer Barpanda^{†#§} and Gopalakrishnan Sai Gautam^{*‡}

[†]Faraday Materials Laboratory (FaMaL), Materials Research Centre, Indian Institute of Science, Bangalore 560012, India.

[‡]Department of Materials Engineering, Indian Institute of Science, Bengaluru, Karnataka 560012, India.

[#]Helmholtz Institute Ulm (HIU), Electrochemical Energy Storage, Ulm 89081, Germany.

[§]Institute of Nanotechnology, Karlsruhe Institute of Technology (KIT), Karlsruhe 76021, Germany.

***Corresponding Author; E-mail: saigautam@iisc.ac.in**

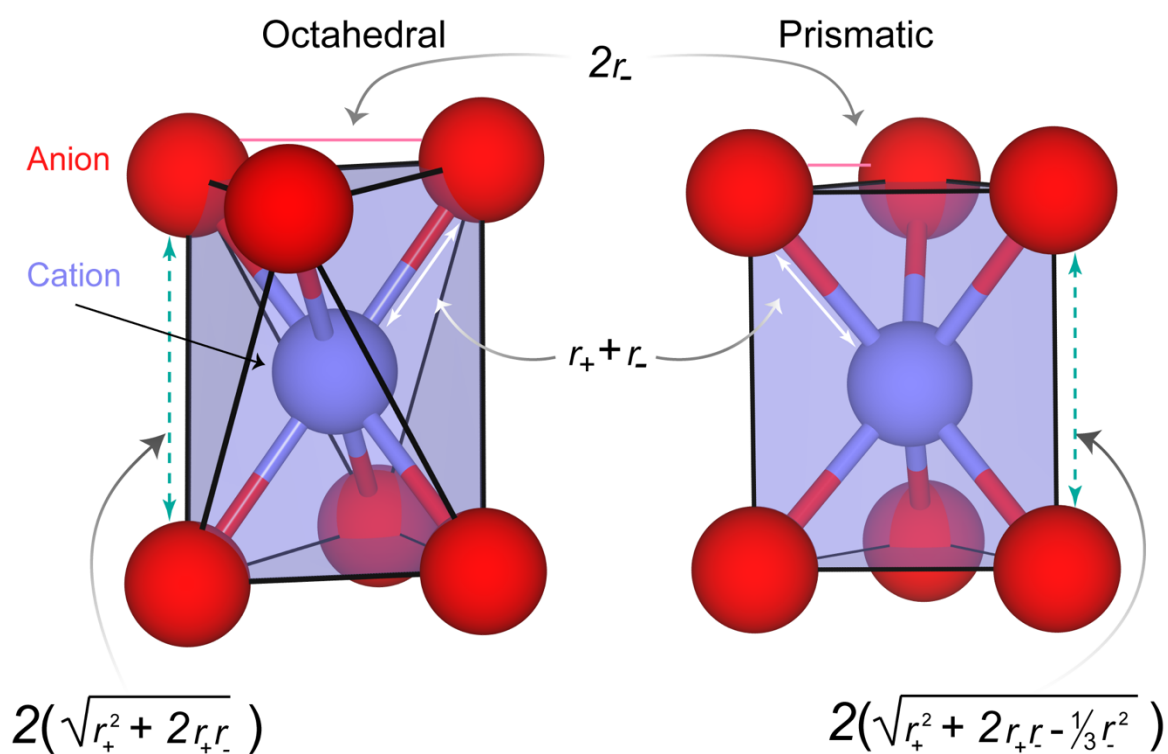


Figure S1. Regular octahedral and prismatic coordinates of K^+ in layered oxides. Specific bond distances and edge lengths are denoted by arrows. Blue and red spheres indicate K and O atoms, respectively. r_+ and r_- indicate Shannon crystal radii of K and O, respectively.¹

Table S1: SCAN+ U calculated total energy per formula unit (f.u.) for various magnetic configurations in P3-K_{0.5}CoO₂.

Composition	Ordering	Total energy (eV/f.u.)
K _{0.5} CoO ₂	Anti-ferromagnetic	-37.293
	High spin ferromagnetic	-37.052
	Low spin ferromagnetic	-37.515

Table S2. Calculated lattice parameters of P3-K_{0.5}TMO₂ (TM=transition metals; Ti, V, Cr, Mn, Co, or Ni) using the Hubbard U corrected strongly constrained and appropriately normed (SCAN+ U) functional within the framework of density functional theory (DFT). The available experimental (Expt.) values are also listed for comparison.

System	Source	a (Å)	b (Å)	c (Å)	α (°)	β (°)	γ (°)	Volume (Å ³)
K _{0.5} TiO ₂	DFT	3.06	3.05	21.72	64.64	90.27	120.21	152.43
K _{0.5} VO ₂	DFT	3.03	2.93	21.50	65.99	89.89	121.15	143.40
K _{0.5} CrO ₂	DFT	2.91	2.91	19.66	89.93	90.08	120.00	137.72
	Expt.	2.92	2.92	18.44	90	90	120	136.16
K _{0.5} MnO ₂	DFT	3.01	3.01	18.88	92.01	87.97	123.13	142.82
	Expt.	2.88	2.88	19.08	90	90	120	137.05
K _{0.5} CoO ₂	DFT	2.81	2.81	21.06	66.35	89.75	119.83	127.87
	Expt.	2.83	2.83	18.46	90	90	120	128.04
K _{0.5} NiO ₂	DFT	2.86	2.77	21.04	66.71	88.06	118.90	128.90

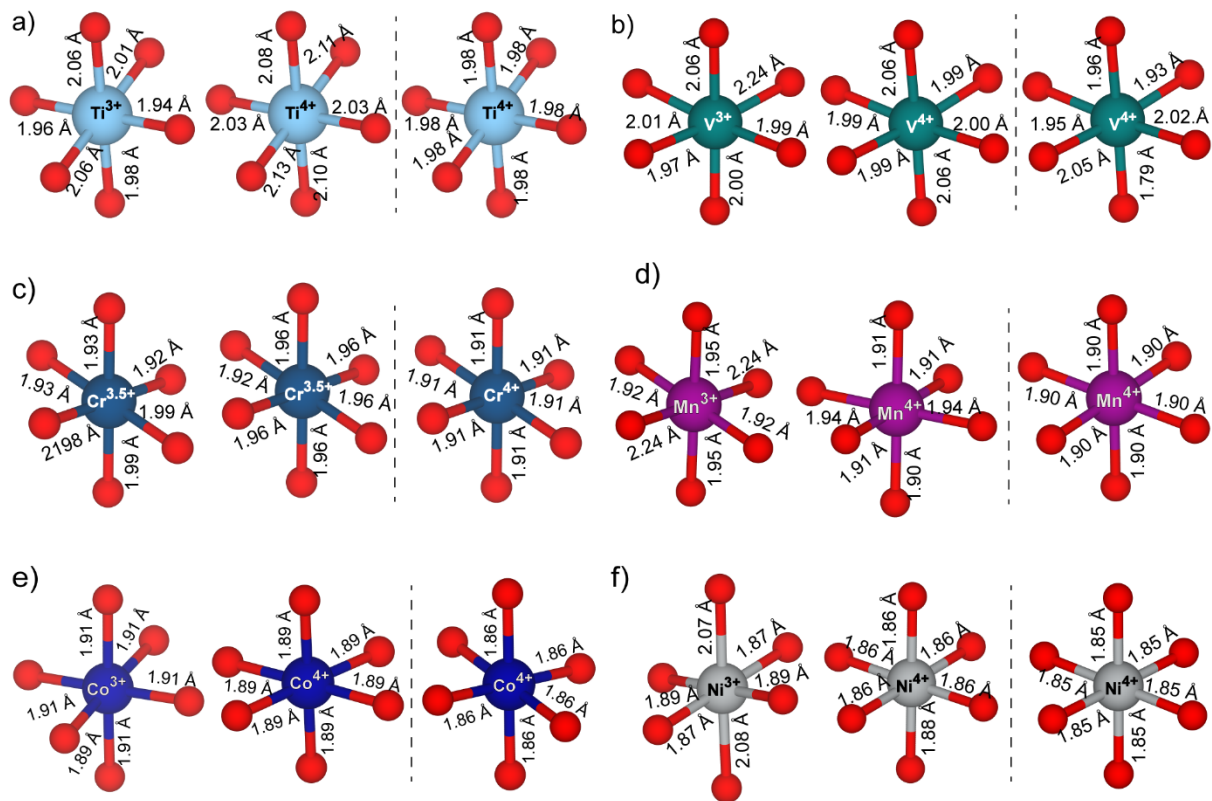


Figure S2. SCAN+*U*-calculated TM-O bond lengths in potassiated (left of dashed lines in each panel) and depotassiated states (right of dashed lines) of a) Ti, b) V, c) Cr, d) Mn, e) Co, and f) Ni P3 frameworks. Red spheres are oxygen atoms.

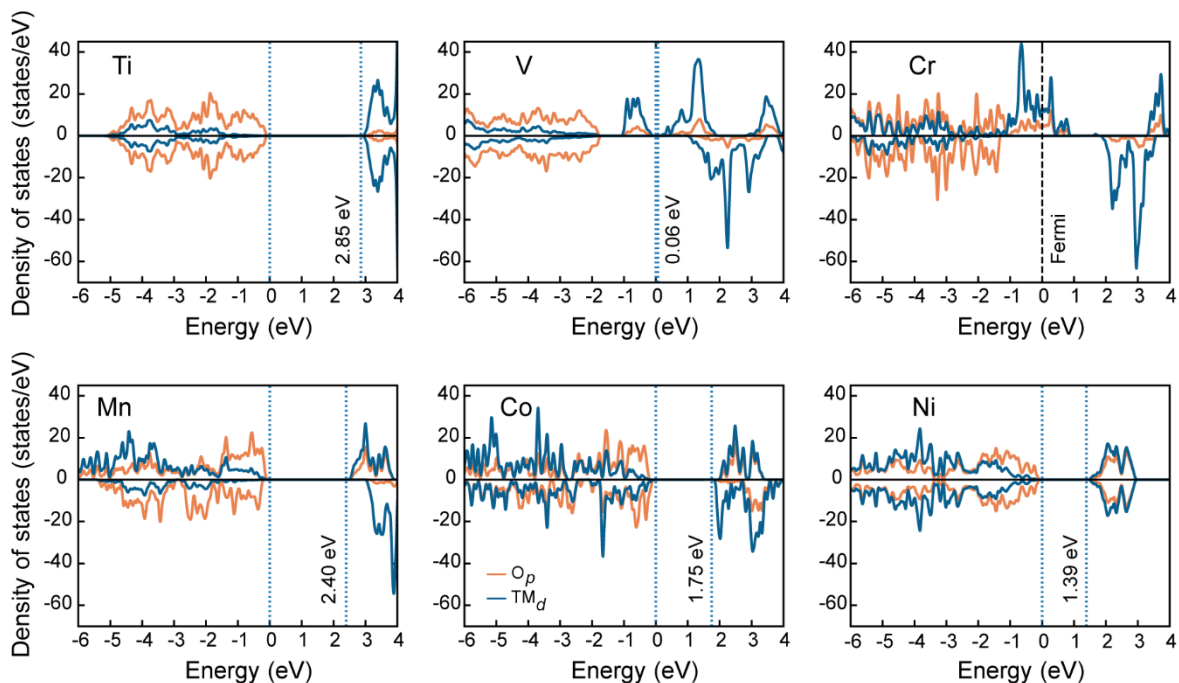


Figure S3. SCAN+*U* calculated projected density of states (pDOS) for depotassiated P3-TMO₂ structures. The notations in each panel are identical to those used in **Figure 3** of the main text.

Table S3. SCAN+*U* calculated on-site magnetic moments of TMs in P3-K_{0.5}TMO₂ and P3-TMO₂. The oxidation state corresponding to each calculated on-site magnetic moment is indicated in parenthesis next to each magnetic moment. All magnetic moments are in units of μ_B . The metallic nature of K_{0.5}CrO₂ prevents distinct identification of Cr³⁺ and Cr⁴⁺ ions within the structure.

TM	Calculated on-site magnetic moments	
	K _{0.5} TMO ₂	TMO ₂
Ti	0.88 (3 ⁺) & 0.06 (4 ⁺)	0.00 (4 ⁺)
V	1.74 (3 ⁺) & 1.16 (4 ⁺)	1.15 (4 ⁺)
Cr	2.51 (3 ⁺ /4 ⁺)	2.24 (4 ⁺)
Mn	3.84 (3 ⁺) & 3.03 (4 ⁺)	3.07 (4 ⁺)
Co (Low spin)	0.01 (3 ⁺) & 1.00 (4 ⁺)	1.06 (4 ⁺)
Ni (Low spin)	0.99 (3 ⁺) & -0.01 (4 ⁺)	0.00 (4 ⁺)

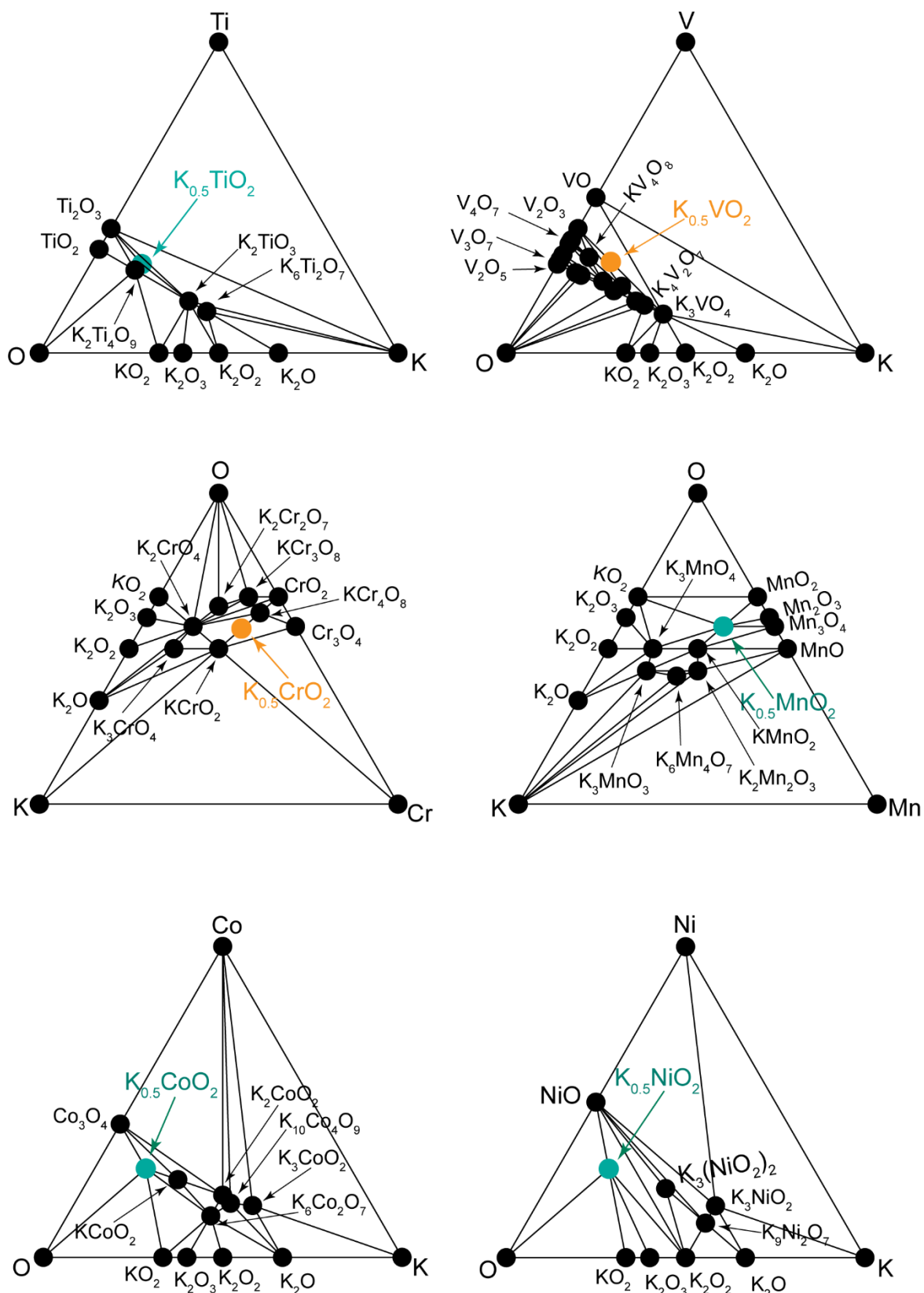


Figure S4. SCAN+*U* calculated 0 K K-TM-O ternary phase diagrams. All the stable compositions within the phase diagram are indicated by solid black circles. Solid black lines are tielines. The P3- $K_{0.5}TMO_2$ compositions of interest are identified either by solid green (stable) or solid orange (metastable) circles.

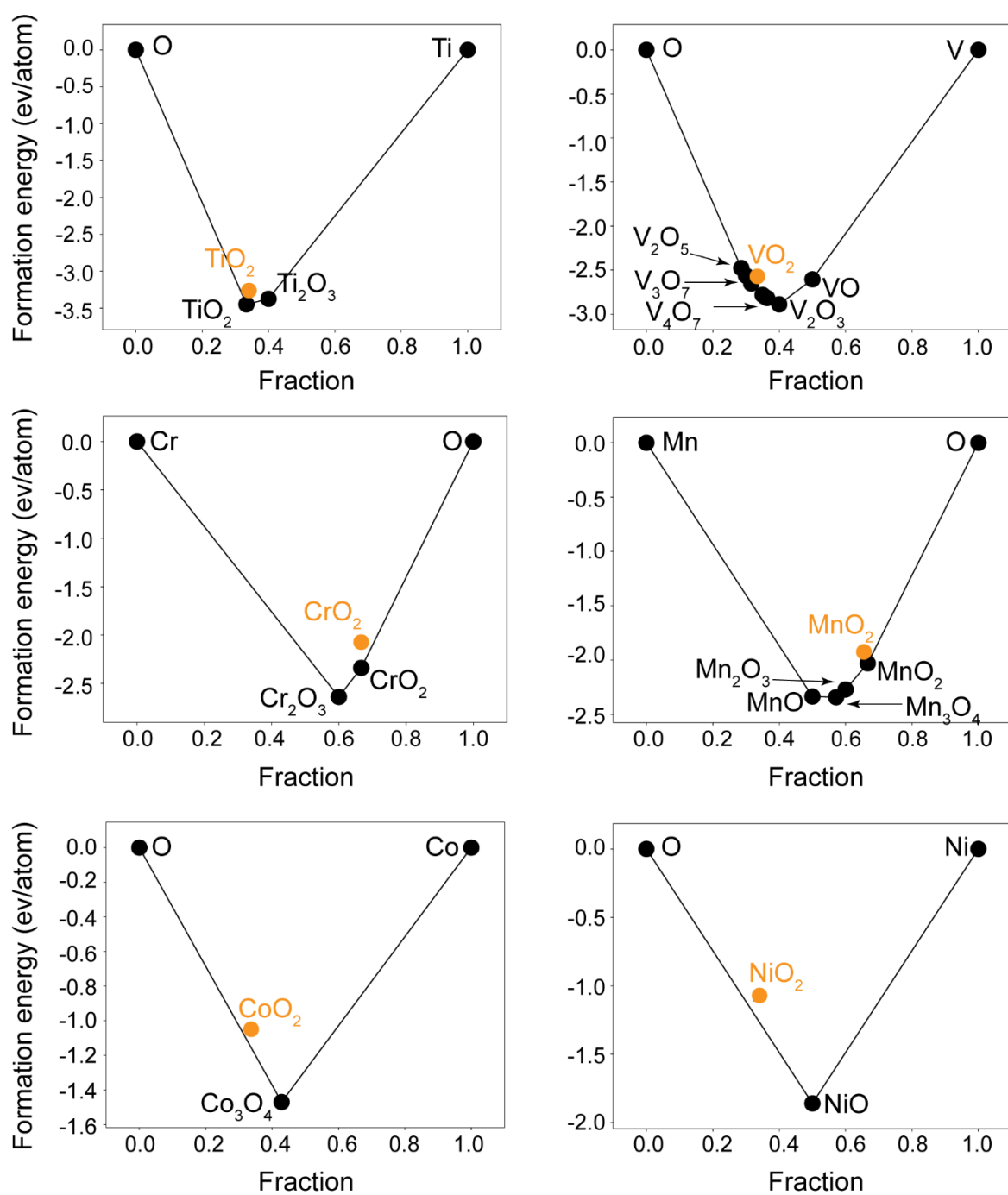


Figure S5. SCAN+*U* calculated 0 K TM-O binary phase diagrams. Depotassiated P3-TMO₂ compositions are indicated by solid orange circles (unstable).

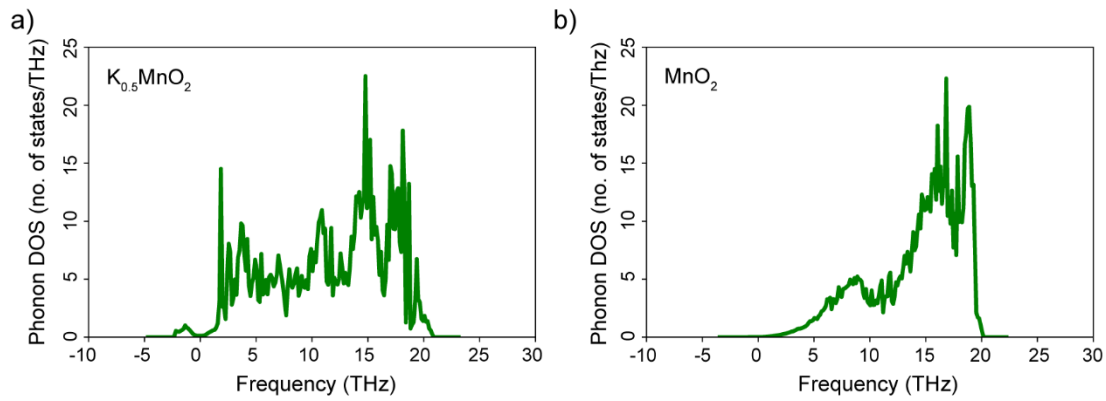


Figure S6. SCAN+ U calculated phonon density of states (DOS) for the a) P3- $K_{0.5}MnO_2$ and b) P3- MnO_2 structures. Negative frequencies correspond to imaginary phonon modes.

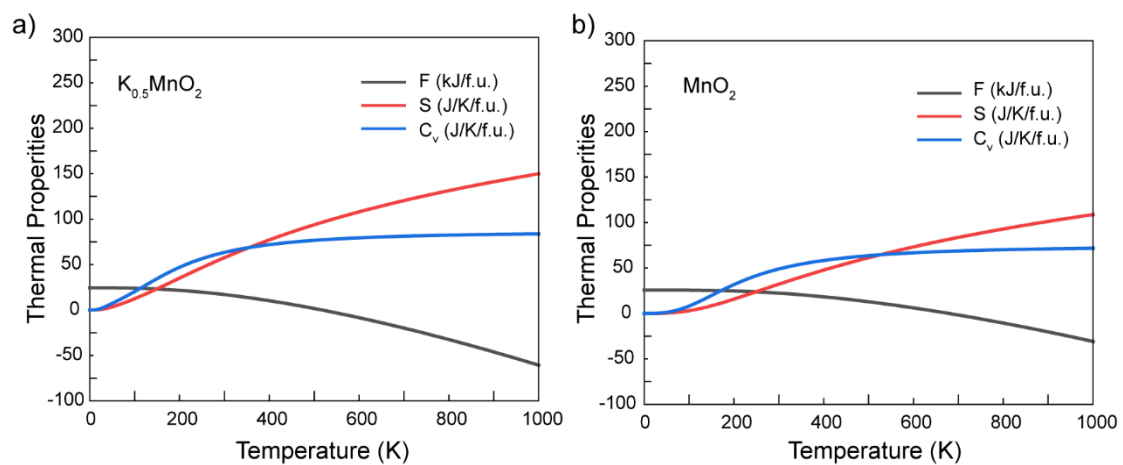


Figure S7. SCAN+ U calculated thermal properties of the potassiated (P3- $K_{0.5}MnO_2$, panel a) and depotassiated (P3- MnO_2 , panel b) based on phonon calculations. The Helmholtz energy (F), entropy (S), and specific heat at constant volume (C_v) are plotted as functions of temperature. Imaginary phonon modes were ignored in calculating the thermal properties.

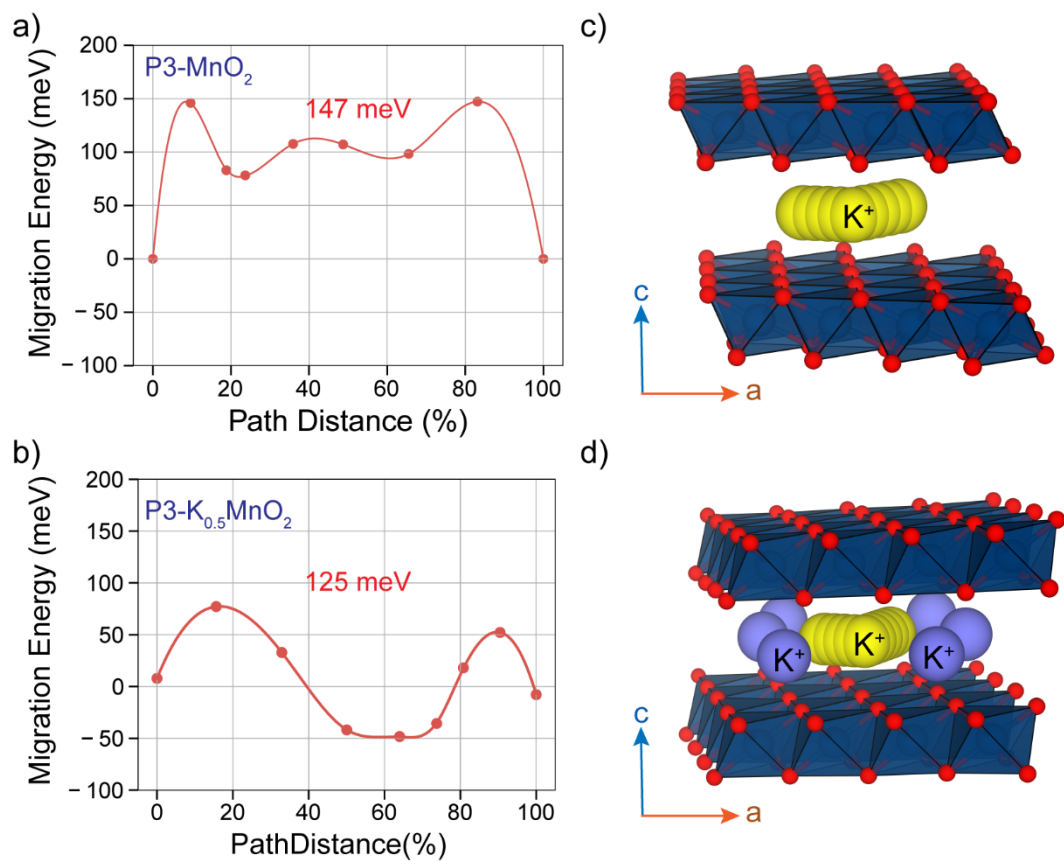


Figure S8. SCAN-calculated minimum energy pathway traced by K^+ and the corresponding migration energy barrier (E_m) in a) $P3-MnO_2$ (top panels) and b) $P3-K_{0.5}MnO_2$ (bottom panels). c-d) Visualization of K^+ migration across equivalent prismatic sites.

Rouxel Diagram

Rouxel diagram measures the extent of ionic-covalent character of the crystal quantifying intercalant radius vs β , according to the equation below:

$$\beta = xf(K - O)f(TM - O) \quad (S1)$$

where,

$$f(TM - O) = 1 - \exp\{-0.25(\chi_{TM} - \chi_O)\}$$

Here, x denotes the potassium content and f accounts for the Pauling bond ionicity of all metal-oxygen bonds, as quantified using the corresponding Pauling electronegativity (χ) difference (see **Table S4**²). Note that in Rouxel diagram classification K-content, bonding between K-O, and bonding between TM-O are important factors in determining the stacking sequence of the structure. The critical value of β for a K-based system is ~ 0.46 which separates octahedral and prismatic frameworks (see **Figure 5a** in main text).

Table S4. Pauling's electronegativity values of the typical elements considered in this study.

Elements	Electronegativity
K	0.82
O	3.44
Sc	1.36
Ti	1.54
V	1.63
Cr	1.66
Mn	1.55
Fe	1.83
Co	1.88
Ni	1.92

Table S5. Calculated β values from **Equation S1** for different K_xTMO_2 systems at different x .

Transition Metals	$x=1$	$x=0.75$	$x=2/3$	$x=0.5$	$x=1/3$	$x=0.25$
Sc	0.5421	-	-	-	-	-
Ti	0.4876	0.3657	0.3251	0.2438	0.1625	0.1219
V	0.4586	0.3440	0.3057	0.2293	0.1529	0.1147
Cr	0.4488	0.3366	0.2992	0.2244	0.1496	0.1122
Mn	0.4844	0.3633	0.3229	0.2422	0.1615	0.1211
Fe	0.3912	0.2934	0.2608	0.1956	0.1304	0.0978
Co	0.3738	0.2804	0.2492	0.1869	0.1246	0.0935
Ni	0.3599	0.2699	0.2399	0.1799	0.1199	0.0899

Cationic potential

Cation potential (Φ_{cation} , **Equation S2**) is based on the mean ionic potentials of individual cations ($\bar{\phi}_{TM}$ and $\bar{\phi}_K$, **Equations S3 and S4**). For an individual TM, its mean cationic potential is the ratio of its oxidation state (n) to its ionic radius (R , typically taken for a 6-coordinated geometry in layered transition metal oxides). For a TM with multiple oxidation states in a given K_xTMO_2 composition (e.g., $K_{0.5}TMO_2$ has equal amounts of TM^{3+} and TM^{4+}), $\bar{\phi}_{TM}$ is the weighted average of individual mean TM cationic potentials, with the corresponding content of a given TM oxidation state (w_i) acting as the weight for that state. Thus, $\bar{\phi}_{TM}$ in $K_{0.5}TMO_2$ will be the arithmetic average of the corresponding $\bar{\phi}_{TM}$ values in $KTMO_2$ (TM^{3+}) and TMO_2 (TM^{4+}). Since the oxidation state of K is 1, $\bar{\phi}_K$ for a given K_xTMO_2 composition is simply defined as the ratio of K-content (x) to the K-ionic radius (R_K , for 6-coordinated environment). $\bar{\phi}_O$ is the mean oxygen potential, and is defined as oxygen's oxidation state (2) normalized by its anionic radius (R_O , in 6-coordination), given that oxygen content is always considered to be 1. **Table S6** compiles the values used to calculate all mean ionic potentials,²⁻⁴ while **Table S7** lists the calculated ionic potentials for several K_xTMO_2 systems, with different K-content (x) and TM. The variation of ϕ_{cation} is plotted against $\bar{\phi}_K$ in **Figure 5b** of the main text.

$$\Phi_{cation} = \frac{\bar{\phi}_{TM} \bar{\phi}_K}{\bar{\phi}_O} \quad (S2)$$

$$\bar{\phi}_{TM} = \sum_i \frac{w_i n_i}{R_i} \quad (S3)$$

$$\bar{\phi}_K = \frac{x}{R_K} \quad (S4)$$

Table S6. Charge and ionic radius (nm) of all elements considered in this study. All ionic radii listed are for 6-coordination. We used the ionic radii corresponding to low spin configuration for Co^{3+} and Ni^{3+} for calculation $\bar{\phi}_{TM}$ since our calculations indicated that Co and Ni adopt the low-spin configurations in $\text{P3-K}_{0.5}\text{TMO}_2$.

Elements	Charge	Ionic radius (nm) High Spin	Ionic radius (nm) Low spin	
K	1 ⁺	0.1380	--	
Sc	3 ⁺	0.0745		
Ti	3 ⁺	0.0670		
	4 ⁺	0.0605		
V	3 ⁺	0.0640		
	4 ⁺	0.0580		
Cr	3 ⁺	0.0615		
	4 ⁺	0.0550		
Mn	3 ⁺	0.0645		0.0580
	4 ⁺	0.0530		--
Fe	3 ⁺	0.0645	0.0550	
	4 ⁺	0.0585	--	
Co	3 ⁺	0.0610	0.0545	
	4 ⁺	0.0530	--	
Ni	3 ⁺	0.0600	0.0560	
	4 ⁺	0.0480	--	

Table S7. Calculated cationic potential and mean ionic potentials of TM, K, and O for K_xTMO_2 compositions, considering different K content (x), and TM.

System	$\bar{\Phi}_{TM}$	$\bar{\Phi}_K$	$\bar{\Phi}_O$	Φ_{Cation}
KScO ₂	40.2685	7.2464	28.5714	10.2130
KTiO ₂	44.7761			11.3563
KVO ₂	46.8750			11.8886
KCrO ₂	48.7805			12.3719
KMnO ₂	46.5116			11.7964
KFeO ₂	46.5116			11.7964
KCoO ₂	55.0459			13.9609
KNiO ₂	53.5714			13.5870
K _{0.75} TiO ₂	50.1110	5.4348		9.5320
K _{0.75} VO ₂	52.3976			9.9670
K _{0.75} CrO ₂	54.7672			10.4177
K _{0.75} MnO ₂	53.7516			10.2245
K _{0.75} FeO ₂	51.9777			9.8871
K _{0.75} CoO ₂	60.1523			11.4420
K _{0.75} NiO ₂	60.0119			11.6055
K _{2/3} TiO ₂	51.8893			4.8309
K _{2/3} VO ₂	54.2385	9.1708		
K _{2/3} CrO ₂	56.7627	9.5976		
K _{2/3} MnO ₂	56.1650	9.4965		
K _{2/3} FeO ₂	53.7998	9.0966		
K _{2/3} CoO ₂	61.8545	10.4585		
K _{2/3} NiO ₂	63.4921	10.7354		
K _{0.5} TiO ₂	55.4459	3.6232		
K _{0.5} VO ₂	57.9203			7.3450
K _{0.5} CrO ₂	60.7539			7.7043
K _{0.5} MnO ₂	60.9917			7.7345
K _{0.5} FeO ₂	57.4438			7.2845
K _{0.5} CoO ₂	65.2588			8.2756
K _{0.5} NiO ₂	68.4524			8.6806
K _{1/3} TiO ₂	59.0025			2.4155
K _{1/3} VO ₂	61.6020	5.2079		
K _{1/3} CrO ₂	64.7450	5.4736		
K _{1/3} MnO ₂	65.8183	5.5644		
K _{1/3} FeO ₂	61.0879	5.1644		
K _{1/3} CoO ₂	68.6631	5.8049		
K _{1/3} NiO ₂	73.4127	6.2064		
K _{0.25} TiO ₂	60.7808	1.8116		
K _{0.25} VO ₂	63.4429			4.0226
K _{0.25} CrO ₂	66.7406			4.2317
K _{0.25} MnO ₂	68.2317			4.3263
K _{0.25} FeO ₂	62.9099			3.9889
K _{0.25} CoO ₂	70.3652			4.4616
K _{0.25} NiO ₂	75.8929			4.8120

References

1. R. D. Shannon, Revised Effective Ionic Radii and Systematic Studies of Interatomic Distances in Halides and Chalcogenides. *Acta Crystallogr., Sect. A: Cryst. Phys., Diffr., Theor. Gen. Crystallogr.* 1976, **32**, 751–767.
2. L. Pauling, *The Nature of the Chemical Bond* (Cornell Univ. Press, ed. 3, **1960**).
3. L. Pauling, The sizes of ions and the structure of ionic crystals. *J. Am. Chem. Soc.*, 1927, **49**, 765–790.
4. C. Zhao, Q. Wang, Z. Yao, J. Wang, B. Sánchez-Lengeling, F. Ding, X. Qi, Y. Lu, X. Bai, B. Li, H. Li, A. Aspuru-Guzik, X. Huang, C. Delmas, M. Wagemaker, L. Chen and Y. S. Hu, Rational design of layered oxide materials for sodium-ion batteries. *Science*, 2020, **370**, 708-711.